CONDITIONS FOR HETEROGENEOUS NUCLEATION IN THE PHYSIOLOGICAL ENVIRONMENT

P. Tikuisis and W. R. Johnson

The genesis of bubble formation leading to decompression sickness is a problem that continues to evade many research efforts. Several models of bubble formation have been reviewed (1) and can be summarized by the following classifications: a) de novo formation, b) critical volume concepts, and c) pre-existing gas nuclei. The latter two classifications circumvent the complex question of gas phase separation. Nevertheless, a knowledge of the parameters involved in this de novo event is required to correctly model the growth of the gas phase even if the nucleation itself appears insignificant. In this paper, we examine the conditions under which heterogeneous nucleation (which is thermodynamically favorable over homogeneous nucleation) can occur in the physiological environment.

THEORETICAL DEVELOPMENT

According to classical nucleation theory (2), there is a constant production of gas nuclei in liquids. However, unless a gas nucleus grows beyond the critical size of the liquid-gas solution, the nucleus will dissolve back into solution. The critical size is characterized by the radius, R_c, which is a property of the liquid-gas solution and can be expressed as (3)

$$R_c = 2\gamma/(P^T - P^A), \qquad (1)$$

where γ is the liquid-gas interfacial surface tension, P^T represents the pressure at which the gas phase is in equilibrium with the liquid-gas solution, and P^A is

the ambient pressure. P^T is a composite of the inert gas and any metabolic gases dissolved in the fluid or tissue. We therefore write

$$P^T = P^T_I + P_m, \tag{2}$$

where P^T_I represents the inert component, hereafter referred to as the inert gas tension, and P^T_m is the balance. The inert gas tension can be expressed in terms of the critical radius by combining *Eqs. 1* and *2*, i.e.,

$$P^T_I = P^A - P^T_m + 2\gamma/R_c. \tag{3}$$

The degree of gas saturation, S, is defined as the ratio of the inert gas tension over ambient pressure and therefore becomes

$$S = 1 - P^T_m/P^A + 2\gamma/R_cP^A. \tag{4}$$

To evaluate P^T_m, we consider the *inherent unsaturation* in living tissue, defined as the difference between the ambient pressure and the sum of dissolved gases under conditions of inert gas equilibrium (4). Assuming that the ambient composition comprises of oxygen and the inert gas, the inherent unsaturation can, therefore, be expressed as

$$\Delta p = Po^A_2 - P^T_m, \tag{5}$$

where Po^A_2 is the ambient partial pressure of oxygen. According to the data of Hills and LeMessurier (5)), the inherent unsaturation can be approximated by

$$\Delta p = -P_v + 0.9\, Po^A_2, \tag{6}$$

where P_v is the vapour pressure of water at 37°C. The expression for P^T_m, obtained by combining *Eqs. 5* and *6*, is therefore given by

$$P^T_m = P_v + 0.1\, Po^A_2, \tag{7}$$

which has a value of 0.0084 MPa for aqueous tissue at 37°C and at normal surface conditions.

We now consider the crevice model (6), shown in Fig. 1, for the nucleation of the gas phase. The rate of formation of a critical-sized nucleus, that is, one whose radius of curvature of the liquid-gas interface equals R_c, is given by

$$J = K_N \exp(-\Delta F/kT), \tag{8}$$

where K_N is the rate constant, ΔF is the change in the Helmholtz potential during the formation of the critical sized nucleus, k is the Boltzmann constant and T is the temperature. The rate constant, K_N, is given by (7)

$$K_N = kT(\pi W^3/3h \tan\alpha) \sum_i c_{io}, \tag{9}$$

where W is the radius of the mouth opening of the conical crevice, h is Planck's constant, 2α is the apex angle of the crevice and c_{io} is the initial concentration of the i-th component in liquid-gas solution. The change in the

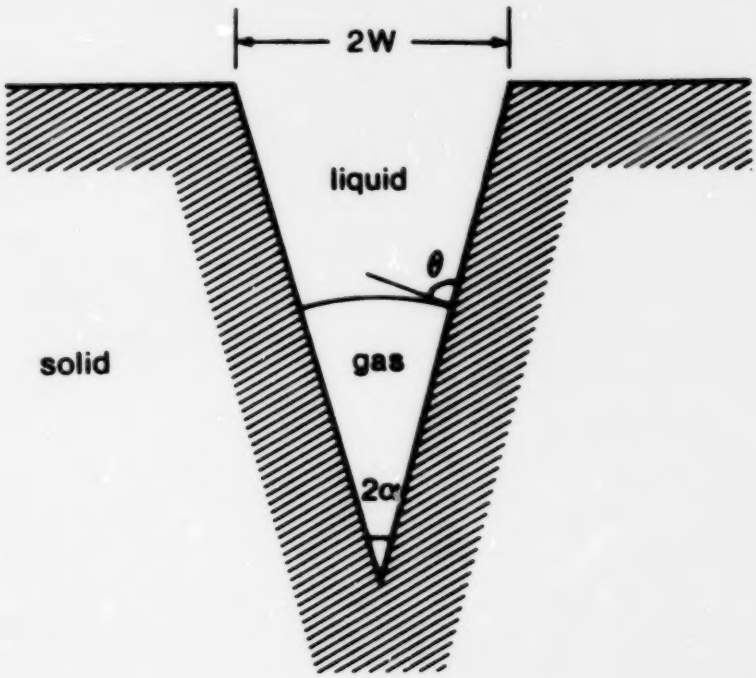

Fig. 1. Schematic of the conical crevice, where 2α is the apex angle, 2W is the diameter of the mouth opening, and θ is the contact angle between the liquid-gas interface and the crevice wall as measured through the liquid. The curvature of the liquid-gas interface of the critical-sized nucleus is defined by the critical radius, R_c, of the liquid-gas solution.

Helmholtz potential during the formation of the critical sized nucleus is expressed by (8)

$$\Delta F = \pi\gamma R_c (-2g_1/3 + 2g_2 + g_3), \tag{10}$$

where $g_1 = 2 - 3\sin(\theta-\alpha) + \sin^3(\theta-\alpha) + \cos^3(\theta-\alpha)\cot\alpha$, (11)

$$g_2 = 1 - \sin(\theta-\alpha), \tag{12}$$

and

$$g_3 = \cos^2(\theta-\alpha)\csc\alpha\cos\theta. \tag{13}$$

The rate of nucleation is quite sensitive to the change in the Helmoltz potential; that is, a small change in ΔF leads to order of magnitude changes in J as defined by *Eq. 8*. The conditions for nucleation are therefore not greatly affected by the rate itself. We choose a rate of 1 to represent the onset of

nucleation in this study. Hence, from *Eqs. 8* and *10*, we obtain the expression of the critical radius for the nucleation of the gas phase in the conical crevice as

$$R_c = \{kT \ln(K_N)/\pi\gamma(-2g_1/3 + 2g_2 + g_3)\}^{1/2}. \quad (14)$$

Substitution of *Eq. 14* into *Eq. 4* will give the expression for the threshold gas supersaturation ratio, S_n, required for the formation of the critical sized nucleus.

RESULTS

We consider a decompression to normal sea level values and assume a constant temperature of 37°C. In this circumstance, the expression for the threshold supersaturation ratio for nucleation, given by *Eq. 4*, becomes

$$S_n = a + b\gamma/R_c, \quad (15)$$

where a equals 0.917 and b equals 19.74 MPa^{-1}.* This reduces the number of parameters of our study to four; namely, the interfacial surface tension γ, the contact angle between the liquid-gas interface and the solid-gas interface as measured through the liquid, θ, the radius of the crevice opening, W, and the apex angle in the crevice, 2α. The logarithmic dependence of R_c upon W, through the rate constant K_N, is small and therefore the dependence of S_n upon W is also small. The importance of W lies with the outgrowth or emergence of the bubble from the crevice, which is discussed further later. We will now examine the effects of the three remaining parameters on the value of S_n.

Figure 2 shows the values of S_n plotted against θ for various values of γ. Although W and α are chosen to have values of 1.0 μm and 2°, respectively, the results are representative of the general dependence of S_n upon γ. Low levels of gas supersaturation are required for heterogeneous nucleation only if γ is small. Substances such as lung surfactant exhibit low values of γ (10), but are not considered to be a "bulk" fluid. For more common fluids such as plasma, whose surface tension is about 50 dynes/cm, the sensitivity of S_n upon θ is such that heterogeneous nucleation at modest gas supersaturations could only occur if the surface is hydrophobic, that is, for values of θ of 90° or greater. Note that for a half apex angle of 2°, the curvature of the liquid-gas interface in the crevice remains convex upwards, as shown for example in Fig. 1, for contact angles of less than 92°. This is true in general provided that the difference, $\theta - \alpha$, is less than 90°. If this difference approaches 90°, as is

*At high ambient pressures, the term P_n^T/P^A in *Eq. 4* becomes negligible and therefore the value of a can be approximated by unity. In this circumstance, it can be shown that our model predicts that heterogeneous nucleation requires a specific difference between the gas tension and the ambient pressure and that this difference is independent of the ambient pressure. This feature is also characteristic of homogeneous nucleation (9).

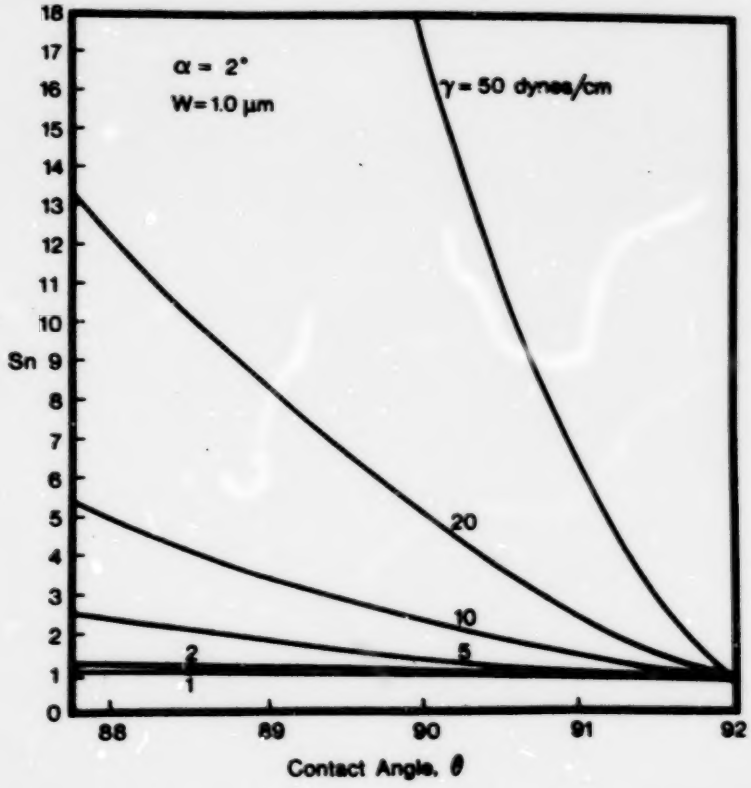

Fig. 2. Threshold gas supersaturation ratio, S_n, required for heterogeneous bubble nucleation as plotted against the contact angle, θ, for various values of the interfacial surface tension, γ; for a crevice with one-half the apex angle, α, equal to 2°; and a mouth opening of radius, W, equal to 1.0 μm.

shown in Fig. 2 for θ approaching 92°, then the liquid-gas interface becomes flat. Consequently, the Laplace pressure term, $2\gamma/R_c$, becomes unimportant and all curves of varying γ values converge towards a common point, that is, towards the value of α in *Eq. 15*. If the difference, $\theta - \alpha$, exceeds 90°, then the crevice will maintain a gas nucleus whose curvature is concave upwards. Such a configuration is thermodynamically stable under any degree of gas saturation (7), hence, the stabilizing mechanism for "pre-existing" gas nuclei, and theoretically provides a ready source for the formation of gas bubbles upon gas supersaturation. The only barrier to the emergence of such bubbles is the extent of the crevice mouth opening, which we consider further below.

The dependence of S_n upon α, shown in Fig. 3, is determined by the contact angle θ. If the contact angle equals or exceeds 90°, then the value of

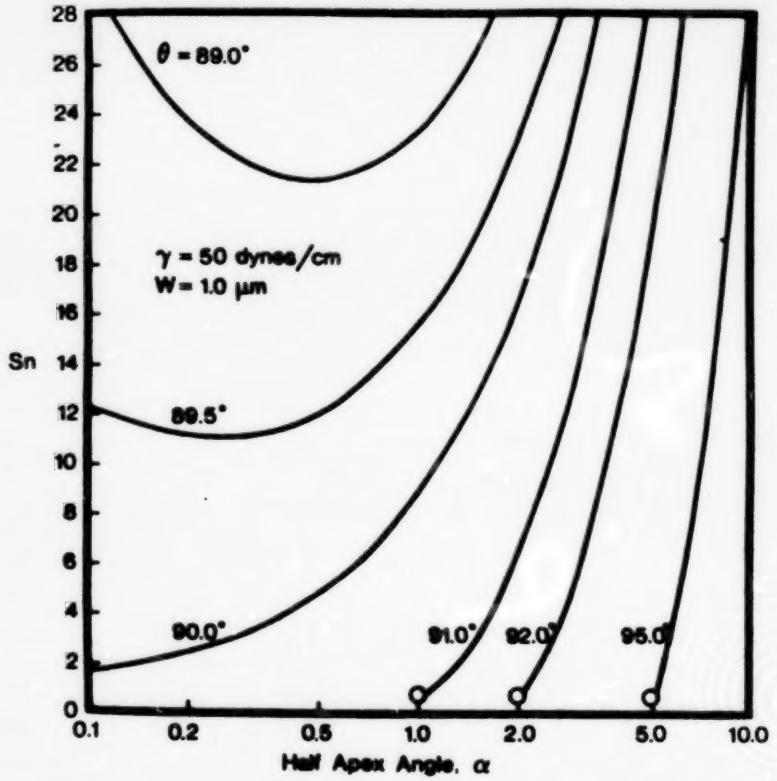

Fig. 3. Threshold gas supersaturation ratio, S_n, required for heterogeneous bubble nucleation as plotted against one-half the apex angle, α, for various values of the contact angle, θ; for an interfacial surface tension, γ, equal to 50 dynes/cm; and a crevice with a mouth opening of radius, W, equal to 1.0 μm.

S_n is reduced by decreasing the apex angle. The *open circles* in Fig. 3 indicate the point at which the liquid-gas interface becomes flat. For contact angles of value less than 90°, there is a minimum value of the threshold gas supersaturation ratio for nucleation, which can be determined by differentiating the expression for S_n by α and equating the result to zero. In essence, this minimum value of S_n increases rapidly as the contact angle decreases in value from 90°.

Finally, we consider the emergence of a bubble from a crevice. Once the gas nucleus reaches the mouth of the crevice, the radius of the liquid-gas interface begins to decrease. This radius continues to decrease until a minimum is reached whose value is equal to the radius of the mouth opening of the crevice, i.e., W. This constraint imposes a minimum gas supersaturation

ratio for the emergence of the nucleated bubble denoted as S_g and is expressed by

$$S_g = a + b\gamma/W. \quad (16)$$

Accordingly, this added constraint for bubble formation is not affected by either θ or α. Depending upon the value of W, however, the value of S_g may be less or greater than the threshold requirement for nucleation. This can be better appreciated by comparing the predictions from *Eqs. 15* and *16*. For example, for an interfacial surface tension of 20 dynes/cm, a contact angle of 90°, an apex angle of 5°, and a crevice mouth opening of 0.2 μm, the value of S_n is 6.31, according to *Eq. 15*, and the value of S_g is 4.86, according to *Eq. 16*. In this circumstance, the threshold gas supersaturation ratio for nucleation exceeds the supersaturation ratio required for the emergence of the bubble; hence, bubble production in this instance requires only that the nucleation threshold be met. On the other hand, if the crevice mouth opening is halved to 0.1 μm while maintaining the other parameters unchanged, then S_g increases to 8.81, whereas S_n increases only slightly to 6.42. Therefore, although the conditions for heterogeneous nucleation may be met in this circumstance, the bubble will not appear unless the gas supersaturation ratio exceeds 8.81. Consequently, a gas bubble may form and remain stabilized within the crevice until the ambient conditions alter, i.e., further decompression, to promote the emergence of a bubble. Figure 4 shows the gas supersaturation ratio required for the emergence of the bubble plotted against W for various values of the interfacial surface tension.

It is instructive to note the geometric relationship between α and W. On the one hand, heterogeneous nucleation is enhanced for small values of α; however, for the emergence of the bubble the crevice mouth opening cannot be too small. Thus, the most favored geometry for bubble formation is a narrow yet deep conical crevice.

DISCUSSION

The formation of gas bubbles in decompressed rats is believed to occur where the gas supersaturation ratio might be as small as 3 or 4 (11) and has been observed in guinea pigs for a gas supersaturation ratio as low as 1.69 (12). We view the results described previously as prescribing a very specific set of constraints for which heterogeneous bubble nucleation and bubble emergence can occur in the physiological environment for these ratios. Our results indicate that

1) θ must be 90° or greater;

2) α must be small, certainly less than 5°;

3) γ must be relatively low compared to the interfacial surface tension value between water and air; and

4) W must be of the order of 0.1 μm (greater if γ is large).

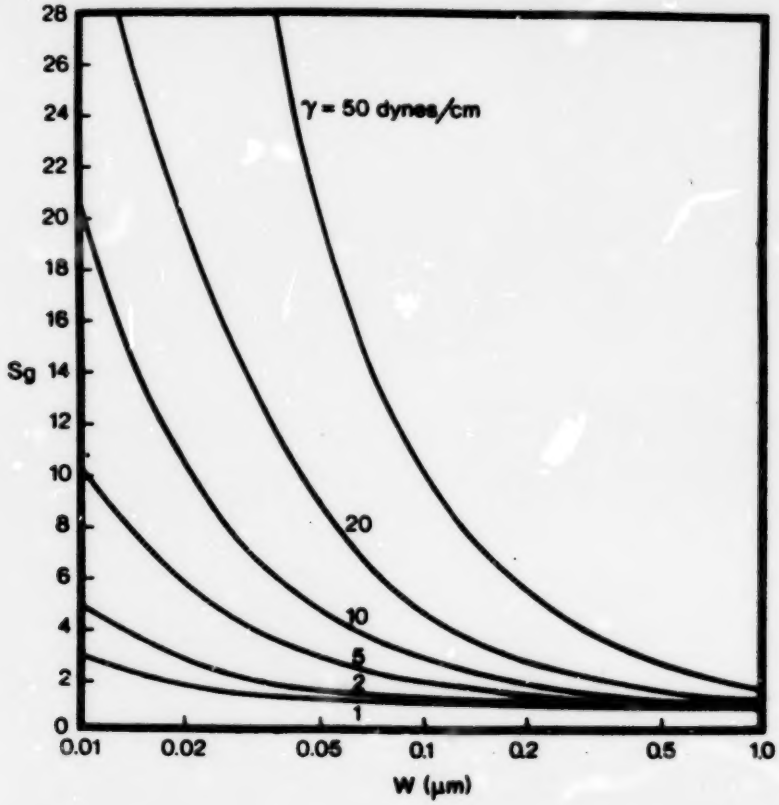

Fig. 4. Threshold gas supersaturation ratio, S_g, required for the emergence of a bubble as plotted against the radius of the crevice mouth opening, W, for various values of the interfacial surface tension, γ.

These conditions restrict the search for potential nucleation sites to hydrophobic surfaces forming exceptionally rough geometries that are characterized by subcellular dimensions. Thus, our attention is focused not on cellular surfaces per se, but on intercellular components, and points of cellular contact.

The "ruffled" surface geometry of certain subcellular components closely satisfies the requirements for heterogeneous nucleation as predicted by our model. For example, the membrane of mitochondria is an undulating lipid surface whose crevices have mouth openings typically less than 0.2 μm in radius and apex angles less than 2° (13). For an interfacial surface tension value of 50 dynes/cm, heterogeneous nucleation could readily occur in a conical crevice having this geometry when the gas supersaturation ratio is between 3 and 4 if the contact angle has a value of about 90.5°. However, in

order for the nucleated bubble to emerge from the crevice with this degree of gas supersaturation, an interfacial surface tension value of between 2 and 5 dynes/cm is required, as determined by *Eq. 16* and shown in Fig. 4. The hypothesis that mitochondria could be a nucleation site is reinforced by the work of Bennett (14).

Still another undulating surface where nucleation might occur is the ruffled border of the membrane of osteoclasts found in bone and represented schematically in Fig. 5. The undulations in this membrane typically have dimensions somewhat larger than those of the subcellular mitochondria (15). Therefore, we expect the gas supersaturation required for heterogeneous nucleation here to be greater than in the previous case. Indeed, for a conical crevice with an apex angle of 6° and mouth opening of 0.2 μm, and assuming a contact angle of 90.5°, our model predicts that gas supersaturation ratios

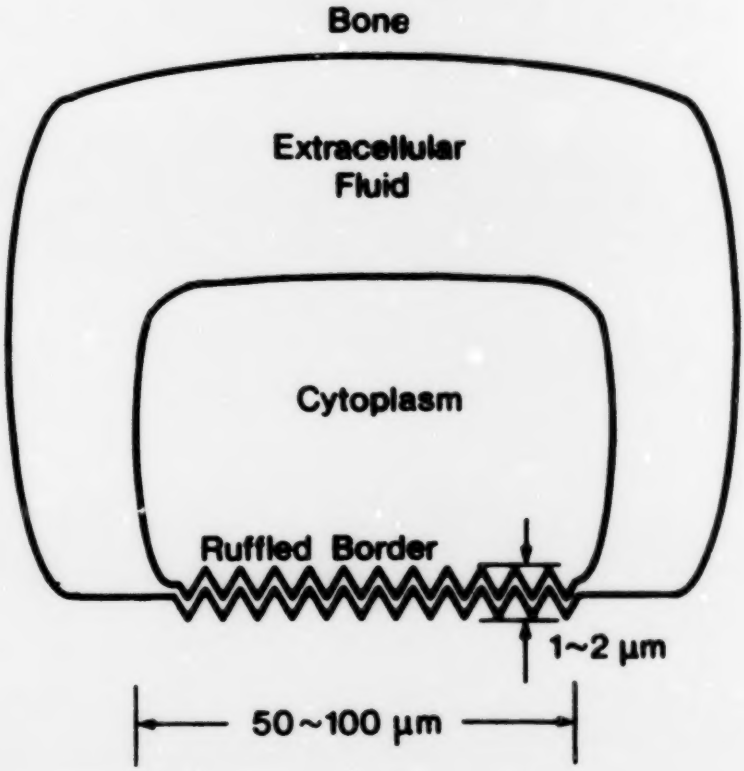

Fig. 5. Schematic of the ruffled border of the osteoclast in close contact with the bone separated by a thin layer of extracellular fluid.

ranging between 1.5 and 20.4 are necessary for interfacial surface tension values ranging between 5 and 50 dynes/cm, respectively. Emergence of the nucleated bubble for these surface tension values require minimum gas supersaturation ratios of 1.9 and 10.8, respectively. Therefore, for the assumed conditions of the ruffled border of the osteoclast, bubble production is governed by the emergence from the crevice if the interfacial surface tension has a value of 5 dynes/cm and is governed by the nucleation threshold if the value is 50 dynes/cm.

Heterogeneous nucleation within the osteoclast may cause sufficient pressure to cause bone damage. This damage could occur because the osteoclast can be modelled essentially as a closed-volume to a rapidly expanding gas bubble. The pressure in the osteoclast, once a bubble has formed, could theoretically rise to nearly the original saturation pressure (8). Therefore, if the cell lies close to the outer surface of the bone, say within a few 10's of micrometers, the bone is then subject to mechanical fracture. This prediction is consistent with recent histological observations of inner-ear bone damage in squirrel monkeys (16). Bone segments were found within the semicircular canals, a finding suggesting that these canals suffered an implosive fracture. This can be accounted for by the forces that originate in the osteoclast cells because of over-pressurization by an expanding bubble.

The required geometry for heterogeneous nucleation can also be realized in the contact between lipid membrane surfaces. Two possible candidates may be found in the Rouleaux formation of red blood cells and in the contact between adjoining cells such as those in the endothelium. In such instances where the conical crevice geometry may be present, the apex angle approaches zero at the contact point and the probability of heterogeneous nucleation at a given gas supersaturation increases. This readily can be seen in Fig. 3. The possibility of bubble emergence, however, is not exactly clear. This is exemplified in Fig. 4 where we have observed that the narrower the crevice mouth opening, the less likely will the bubble emerge. The emergence of the bubble may be resolved, however, if during the nucleation process, a distortion of the malleable cells takes place and in turn the geometry of their contact is altered in such a manner as to increase the crevice mouth opening. Thus, on one hand, close contact of cells will enhance the nucleation process, yet, on the other hand, their separation will favor emergence of the nucleated bubble. The exact mechanism for the distortion of the cells is undoubtedly complex for while the high pressure of the expanding bubble tends to separate the cells further, the surface tension of interfaces tends to draw the cells together. A bubble stabilized between two cells may emerge if the cells become separated by other means, for instance, when the Rouleaux formation of red blood cells is destroyed upon entering a high shear flow field.

Lastly, the model presented here indicates that in those locations in the physiological environment where the dimensions are quite small, with particular attention to the apex angle, heterogeneous nucleation is more likely to occur and to produce a stable bubble. Some macromolecules such as fibrinogen and globulins have dimensions of several 10's of nanometers. The

shape of these macromolecules in the blood has been investigated by numerous researchers (e.g., Ref. 17) with no definitive conclusion forthcoming. However, if the proponents of the hypothesis that fibrinogen has a convoluted shape are correct, then this particular blood protein would be worthy of investigation as a nucleation site.

In conclusion, heterogeneous nucleation and bubble emergence may readily occur during decompression in certain identifiable locations in the body. The geometrical constraints for nucleation, although severe, are satisfied in ruffled surfaces and lines of contact between surfaces. No less severe are the constraints on the surface tensions and contact angles at the candidate nucleation sites mentioned above. While most surface tensions of biological substances have been measured to be in the 10's of dynes/cm, reports of surface tensions as small as 2 dynes/cm have been reported (10). Contact angles have been measured for certain biological specimens such as bacteria (18), however, measurements for cellular membranes, as addressed in this paper, are virtually nonexistent. To completely understand the phenomena of heterogeneous nucleation and bubble emergence during decompression, one must quantify the two parameters of interfacial surface tensions and contact angle; they deserve more attention than they have received in the past.

Acknowledgment

This study represents DCIEM publication No. 83-P-25.

References

1. Weathersby PK, Homer LD. Current concepts of inert gas exchange and decompression. In: Bachrach AJ, Matzen MM, eds. Underwater physiology VII. Proceedings of the seventh symposium on underwater physiology. Bethesda: Undersea Medical Society, Inc., 1981:687–698.
2. Volmer M. Kinetics of phase formation. In: Bonhoeffer LF, ed. Chemical Reaction: Vol. IV (Translated by Intelligence Dept., AMC F-TS-7068), 1939:139–154.
3. Ward CA, Balakrishnan A, Hooper FC. On the thermodynamics of nucleation in weak gas-liquid solutions. Trans ASME 1970;92:695–704.
4. Hills BA. Decompression sickness. Vol. 1: The biophysical basis of prevention and treatment. Chichester: John Wiley and Sons, 1977:239.
5. Hills BA, LeMessurier DH. Unsaturation in living tissue relative to the pressure and composition of inhaled gas and its significance in decompression theory. Clin Sci 1969;36:185–195.
6. Harvey EN, Barnes DK, McElroy WD, Whiteley AD, Pease PC, Cooper KW. Bubble formation in animals 1. Physical factors. J Cell Comp Physiol 1944;24:1–22.
7. Fisher BA. The fracture of liquids. J Appl Phys 1948;19:1062–1067.
8. Ward CA, Johnson WR, Venter RD, Ho BN, Forest TW, Fraser WD. Heterogeneous bubble nucleation and conditions for growth in a liquid-gas system of constant mass and volume. J Appl Phys 1983;54:1833–1843.
9. Weathersby PK, Homer LD, Flynn ET. Homogeneous nucleation of gas bubbles in vivo. J Appl Physiol: Respir Environ Exercise Physiol 1982;53:940–946.
10. Enhorning G. Pulsating bubble technique for evaluating pulmonary surfactant. J Appl Physiol: Respir Environ Exercise Physiol 1977;43:198–203.

11. Vann RD, Grimstad J, Nielsen CH. Evidence for gas nuclei in decompressed rats. Undersea Biomed Res 1980;7:107–112.
12. Daniels S, Eastaugh KC, Paton WDM, Smith EB. Saturation air dives: A threshold for bubble formation. Undersea Biomed Res 1982; 7(Suppl):A24.
13. Ham AW. Histology. 6th ed. Philadelphia: J. B. Lippincott, 1969:153–156.
14. Bennet RA. Fine structure of decompression sickness. In: Shilling CW, Beckett MW, eds. Underwater physiology VI. Proceedings of the sixth symposium on underwater physiology. Bethesda, MD: Federation of American Societies for Experimental Biology, 1978:595–599.
15. Ham AW. Histology. 6th ed. Philadelphia: J. B. Lippincott, 1969:407–411.
16. Landolt JP, Money KE, Topliff EDL, Nicholas AD, Laufer J, Johnson WH. Pathophysiology of inner ear dysfunction in the squirrel monkey in rapid decompression. J Appl Physiol: Respir Environ Exercise Physiol 1980;49:1070–1082.
17. Marguerie G. The shape of the fibrinogen molecule. Thrombos Haemostas (Stuttg) 1979;41:635–670.
18. Neumann AW. Contact angles and their temperature dependence: Thermodynamic status, measurement, interpretation and application. Adv Colloid Interface Sci 1974;4:105–191.

POOR

QUALITY

ORIGINAL